

We are IntechOpen, the world's leading publisher of Open Access books Built by scientists, for scientists

6,900

Open access books available

185,000

International authors and editors

200M

Downloads

Our authors are among the

154

Countries delivered to

TOP 1%

most cited scientists

12.2%

Contributors from top 500 universities



WEB OF SCIENCE™

Selection of our books indexed in the Book Citation Index
in Web of Science™ Core Collection (BKCI)

Interested in publishing with us?
Contact book.department@intechopen.com

Numbers displayed above are based on latest data collected.
For more information visit www.intechopen.com



Surface Nanomechanics of Biomolecules and Supramolecular Systems

Paolo Bergese and Stefania Federici

Additional information is available at the end of the chapter

<http://dx.doi.org/10.5772/intechopen.68293>

Abstract

Surface nanomechanics of biomolecules and supramolecular systems is an interdisciplinary and vital area of current research, with implications/applications spanning from synthetic biology to regenerative medicine, from smart surfaces to molecular machines. Biomolecule surface transformations and nanomachinery arise upon “wiring” them onto surfaces and interfaces. Surface confinement of biomolecules is a common feature of biological systems (e.g., cell membranes) and often a mandatory step for translating their properties into real-world applications (e.g., biosensors). On surfaces biomolecules undergo peculiar transformations and interactions which they do not experience in solution. Such unedited effects open challenges in synthetic systems, for example, by altering or hindering the designed/expected property, but also disclose a wealth of opportunities and surprises. Based on our latest research, this chapter will bring fresh excerpts from the field. It will start with an accessible description of thermodynamics of surface nanomechanics of biomolecules and supramolecular systems and then will show how it can be implemented to gain understanding of grow factor cell signaling, to single out small ligands able to inhibit protein misfolding, to measure energetics of surface confined ferritin during iron loading, and to realize a universal probe for ammine-based designer drugs.

Keywords: molecular transformations, surface, nanomechanics, nanomechanical sensors, grow factors, ferritin, abiotic supramolecular receptors, designer drugs

1. Describing and probing molecule collective surface nanomechanics

The section introduces the description of surface molecule transformations by classical interfacial thermodynamics. This will be helpful to better grasp the working principle of nanomechanical sensors, which will be presented in the next subsection. Nanomechanical sensors are

the basic technology used to probe and quantify molecule collective surface nanomechanics. The level of the treatment is kept concise and accessible to a wide readership; those interested in the throughout treatment are redirected to Refs. [1–3].

For simplicity, let us restrict to the case of a solid supported monolayer of proteins that can only switch between two conformational states, A and B. The switch from A to B can be directed by changing the electrolyte (salt) molar concentration of the solution in which the system is immersed. This changes the amount of ions bound to the protein and the Debye-Hückel screening of the charge interactions on the protein, which in turn trigger the exposition to the solution of peptide groups that were buried in conformation A, driving the protein into conformation B.

With the visual help of **Figure 1**, it can be intuitively seen that the switch from state A to state B involves a change of the in-plane interactions between the proteins, because the switch is intertwined with several nanoscale and subnanoscale changes, such as intermolecular distances, surface charge and monolayer thickness. This can be thermodynamically described by an additional surface work that accompanies the surface transformation with respect to the same transformation occurring in “free” solution. In particular, it can be shown [2, 3] that the surface standard molar Gibbs energy, $\Delta_r G_0^\sigma$, of the surface switch from state A to state B is composed by the sum of an excess surface work, w^σ , and the molar Gibbs energy of the same transformation occurring in bulk solution, $\Delta_r G_0^\circ$:

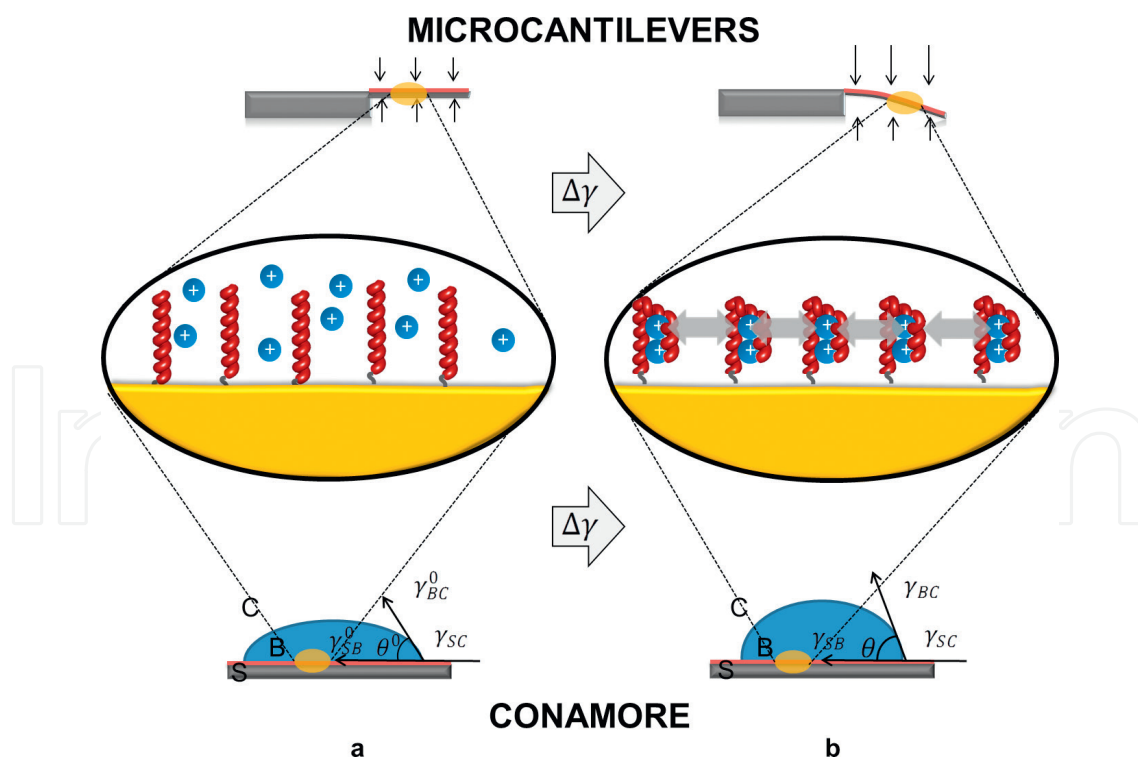


Figure 1. Working principle of nanomechanical sensors in the representative case of a solid supported monolayer of proteins switching between state A (left images) to state B (right images) upon binding to cations. The switch drives the overall variation of surface tension $\Delta\gamma$, triggered at the nanoscale by the change of in-plane interactions between proteins.

$$\Delta_r G_0^\sigma = \Delta_r G_0^b + W^\sigma \quad (1)$$

In addition, W^σ can be further detailed as [2, 3]

$$W^\sigma = \frac{\Delta\gamma}{\Gamma_B} \quad (2)$$

where $\Delta\gamma$ is the thermodynamic surface tension, for simplicity hereafter referred as surface tension, that gathers both the mechanical, $\Delta\sigma$, and electrostatic, ω_e^σ , contributions, and Γ_B is the surface density of proteins in state B. From a (nano)mechanical view point, one can say that $\Delta\gamma$ exerts a surface stress on the surface that supports the molecular monolayer or thin film.

The above considerations and equations have general validity. Molecular transformations, recognition, binding and nanomachinery at a solid-liquid interface involve nano-mechanical work with point of application at the surface. This arises from a very complex co-operative action of electrostatic, steric (hydration) and thermal fluctuation (entropic) forces triggered by the transformation that macroscopically appear as a variation of the surface tension, or the applied surface stress. The nature of the forces is determined by the specific solid-solution interfacial environment, that is, by the molecules and their binding partners, the molecule surface density, the solution composition and ionic strength, the solid surface and modification chemistry, the solid geometry and nanostructure, and so on. This phenomenon is leveraged by static nanomechanical sensors [4]. In particular, the molecular transformations confined on the sensor surface cumulate and perform an overall surface tension change in the order of mN/m [2] that can be probed and translated by tensiometric techniques such as contact angle [5] or microcantilever (MC) beams [6], as sketched in **Figure 1**.

The working principle of MC biosensor is quite simple: the MC surface is functionalized with a receptor that can selectively bind the target species. Adsorption and binding site interactions of the targets change the mechanical response of the MC system (because of the surface stress generated by changes in Gibbs free energy), providing the transduction/sensing mechanism. CONAMORE (COnTact Angle MOlecularREcognition) technique is based on the sessile drop contact angle principle. When a droplet containing the target species is placed onto a solid surface functionalized with a receptor, it reaches equilibrium with the surface and the surroundings under the action of the interfacial tensions at the contact line at which drop, surface, and surroundings meet, forming a definite contact angle [5].

The variation of the overall surface tension $\Delta\gamma$ can be directly determined by CONAMORE measurement, where the molecular transformations can be univocally associated with the differential of the solid-solution interfacial tensions of the systems represented in **Figure 1a** and **b**. In case of MC experiments, $\Delta\gamma$ can be easily calculated through the relation between $\Delta\gamma$ and MC deflection, Δz , given by the Stoney equation [7]:

$$\Delta\gamma = -\frac{\Delta z E t^2}{4 L^2(1-\nu)} \quad (3)$$

where Δz is the cantilever deflection (with the z axis individuated by the unitary vector normal to the top surface of the cantilever base, i.e., $\Delta z < 0$ for a downward cantilever bending), E is the cantilever Young's modulus, t is the cantilever thickness, L is the cantilever length, and ν is the cantilever Poisson's ratio.

Application of nanomechanical sensors to biosensing has become in the last 15 years a breakthrough in biochemistry, life science and medicine, depicting how nanomechanics and biology can grow together [6, 8, 9]. Research in this direction is growing substantially after the milestone work of Fritz and coworkers in 2000, in which they report the specific transduction driven by the surface stress change of DNA hybridization without reported labels [6]. Several experiments have been successfully performed afterwards, revealing DNA hybridization and DNA switch [10–12], detecting proteins and antibodies [5, 13, 14], single virus particles [15] or bacteria [16].

2. Surface nanomechanics of biomolecules

2.1. Role of nanomechanics in the activation of cell membrane growth factors

Ligand-receptor protein interactions are a fundamental mechanism for every biological system, in both physiological and pathological conditions. In particular, the interaction between cell membrane growth factor receptors and their key ligands plays an important role in different processes, including cancer [17]. The growth, survival, and metastatic spreading of solid tumors strongly depend on the formation of a novel vessel network (tumor angiogenesis), making the pro-angiogenic molecular machinery a target for new strategies in cancer therapy [18, 19]. This approach requires to disentangle the complex array of transduction signals activated by the interaction of pro-angiogenic growth factors with their cognate cell membrane tyrosine kinase receptors [20].

In view of this, a nanoliter CONAMORE assay was assessed to investigate the interactions of the vascular endothelial growth factor receptor-2 (VEGFR2), which is the major pro-angiogenic receptor expressed by endothelial cells [21], with the canonical ligand VEGF-A, which is the major pro-angiogenic factor of the VEGF family. The activated complex has a crucial role in physiological and pathological angiogenesis through distinct signal transduction pathways regulating endothelial cell survival, proliferation, migration, vascular permeability, tubulogenesis, and gene expression [22].

The CONAMORE assay scheme and working principle are sketched in **Figure 2**. The recognition between the VEGF-A ligand at nanomolar concentration and the surface confined VEGFR2 was characterized in different scenarios: in the presence of noninteracting proteins, in competitive binding experiments and testing the detection of binding of small peptide ligands to VEGFR2 [23]. In particular, the VEGFR2/VEGF-A recognition was clearly detectable in the presence of a ten-fold molar excess of an unrelated protein (1.0 μ M BSA) and combined with irrelevant immunoglobulins. It was also distinguished from the nonspecific interactions occurring after denaturation of the receptors. The specificity and robustness of the

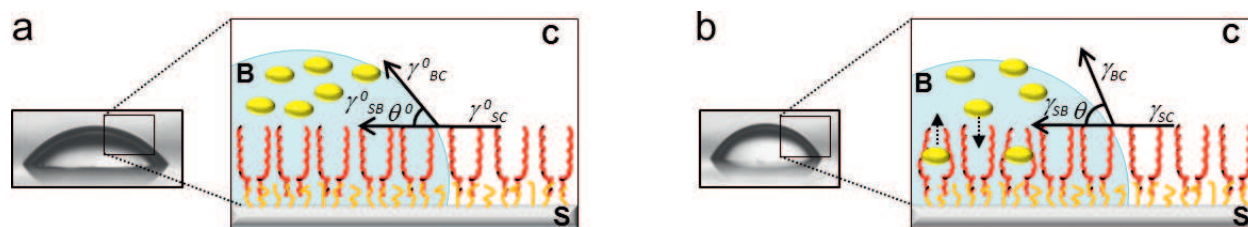


Figure 2. Scheme of the CONAMORE assay in sessile drop configuration for quantification of the nanomachinery of VEGF-A/VEGFR2 surface recognition. (a) Initial state with ligands free in solution. (b) Ligand-receptor recognition equilibrium.

technique were confirmed also by a competition experiment, where the interaction VEGF-A/VEGFR2 was suppressed by a neutralizing anti-VEGF-A antibody, and by a successful detection of an interaction between VEGFR2 and a low molecular weight (LMW) molecule (2 k Dacyclo-peptide).

These preliminary studies set the basis to investigate the role of nanomechanics in the activation of cell membrane growth factors [24]. We started from observations that identified the bone morphogenic protein-antagonist gremlin as a novel pro-angiogenic ligand of VEGFR2, distinct from canonical VEGFs, increasing the complexity of extracellular interactions involving this receptor [24].

VEGF-A/VEGFR2 and gremlin/VEGFR2 surface recognition were first characterized by Surface Plasmon Resonance (SPR) spectroscopy, which is a gold-standard mass-based biosensor [25]. The SPR isotherms of VEGF-A and gremlin overlapped, demonstrating that a similar number of VEGF-A and gremlin molecules interacting with VEGFR2 (VEGF-A and gremlin have very close masses). But, to the contrary, we found the interactions significantly differentiate in terms of binding kinetics and in-plane intermolecular forces, suggesting that the binding of VEGF-A or gremlin induces different VEGFR2 conformational changes and/or clustering in respect to gremlin. Such nanomechanical differences resulted exactly mirrored and supported by the in-vitro experiments. In fact, we showed that VEGF-A triggers a more rapid receptor clustering and a more potent biological response in endothelial cells with respect to gremlin. The key nanomechanical experimental and results are summarized below.

The SPR dose-response experiments were repeated with CONAMORE, by exploiting the fact that with CONAMORE technique is possible to perform the nanomechanical sensing on the same chips used for SPR experiments. **Figure 3a** shows the typical binding curves obtained by plotting $\Delta\gamma_{SB}$ as a function of ligand concentration. In view of the SPR data, the extent of binding of VEGF-A and gremlin matches at any concentration. Therefore, the isotherms indicate that for the same extent of binding to surface-immobilized VEGFR2, VEGF-A exerts a $\Delta\gamma_{SB}$ (blue dots) that is two- to fivefold higher than the $\Delta\gamma_{SB}$ exerted by gremlin (red reverse triangle). At 100 nM, $\Delta\gamma_{SB}$ is (8.3 ± 2.1) mN/m and (3.7 ± 0.4) mN/m for VEGF-A and gremlin, respectively. Remarkably, these values are consistent with MC measurements of cooperative surface mechanical work performed by protein conformational changes [26].

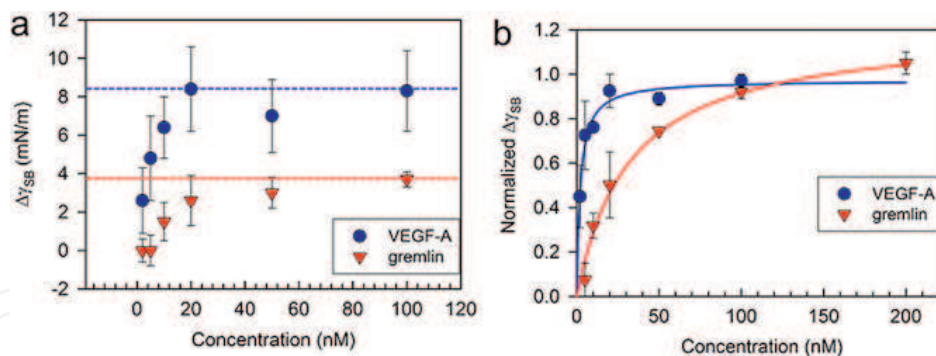


Figure 3. Results of VEGF-A/VEGFR2 and gremlin/VEGFR2 surface recognition. (a) CONAMORE binding isotherms of VEGF-A (blue circles) and gremlin (red reverse triangles) with VEGFR2 immobilized on surface. (b) Normalized $\Delta\gamma_{SB}$ binding isotherms.

Figure 3b shows the normalized $\Delta\gamma_{SB}$ isotherms and the resulting fitting curves with a Langmuir-like equation for monovalent binding. It is possible to estimate an apparent equilibrium constant that explains the nanomechanical aspects of ligand/VEGFR2 surface recognition, named surface nanomechanical affinity, $K_a^{\sigma mech}$, and its reciprocal, $K_d^{\sigma mech} = 1/K_a^{\sigma mech}$, named surface nanomechanical dissociation constant. The VEGF-A isotherm features a sharply steeper rise with respect to the gremlin one, indicating a significant difference in terms of $K_d^{\sigma mech}$. This is supported by the fitting results, which give $K_d^{\sigma mech} = (2.0 \pm 0.7)$ nM and $K_d^{\sigma mech} = (32 \pm 9)$ nM, for VEGF-A and gremlin, respectively. Thus, VEGF-A has about 16-fold higher surface nanomechanical affinity for VEGFR2 with respect to gremlin.

2.2. Nanomechanics and protein folding disorders

Protein conformational changes are a key event in protein's activity, and their characterization is a central goal of biology. Several diseases arise from protein misfolding, in which the misfolded protein self-associates and becomes deposited in amyloid-like aggregates in diverse organs, inducing tissue damage and organ dysfunction.

Beta2-microglobulin ($\beta 2$ -m) is a key protein acting in the onset of the dialysis related amyloidosis (DRA), that is a severe complication occurring in patients subjected to chronic hemodialysis, where insoluble and toxic $\beta 2$ -m amyloid deposits (fibrils) localize in the skeletal tissues [27]. The fibrils formation follows a complex and still unclear mechanism, where protein conformational changes, among other factors, play a crucial role.

MCs biosensors are suited to probe protein conformational changes, as the biomolecular transformation confined on MC surface can be directly translated in MC bending [6]. In particular, silicon MCs with *ad hoc* copolymer coating were employed to probe the effect of an unfolded intermediate of $\beta 2$ -m, driven by pH changes, and in turn to single out within a pilot set of LMW ligands the ones able to influence or even suppress such effect. The working concept is presented in the cartoon in **Figure 4**.

The set of small ligands were selected in order to cover the most relevant scenarios: congo red, a dye that probes fibril formation, speeds up the protein refolding kinetics and can abolish in

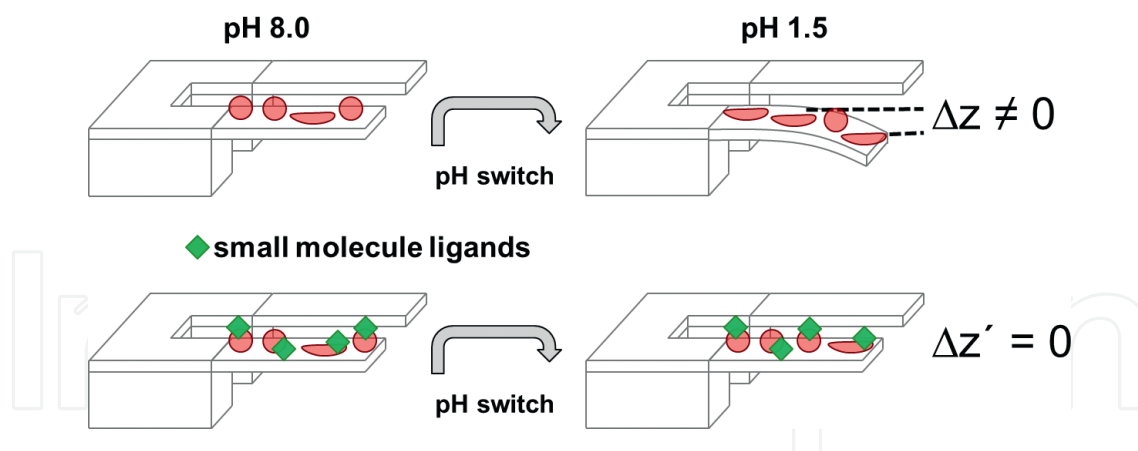


Figure 4. Cartoon representing the effect of small ligands on $\beta 2$ -m conformational stability probed by MC sensors during pH switch. In the top scheme, the pH switch between 8.0 and 1.5 induces a $\beta 2$ -m conformational change that drives MC deflection. In the bottom scheme, the presence of small molecule ligands prevents the protein conformational transformation and in turn MC deflection.

vitro fibril deposition [28], suramin, a urea derivative which also binds the protein but does not interfere with its refolding and without antiamyloid activity [28], and a reference sulfonated molecule that does not bind the protein, hereafter referred as nonbinder.

The pH switch, set between 8.0 and 1.5, drives the MCs functionalized with the native form of $\beta 2$ -m to a mean differential deflection of $\Delta z = (-8 \pm 2)$ nm (**Figure 5** “no ligand”). To test the

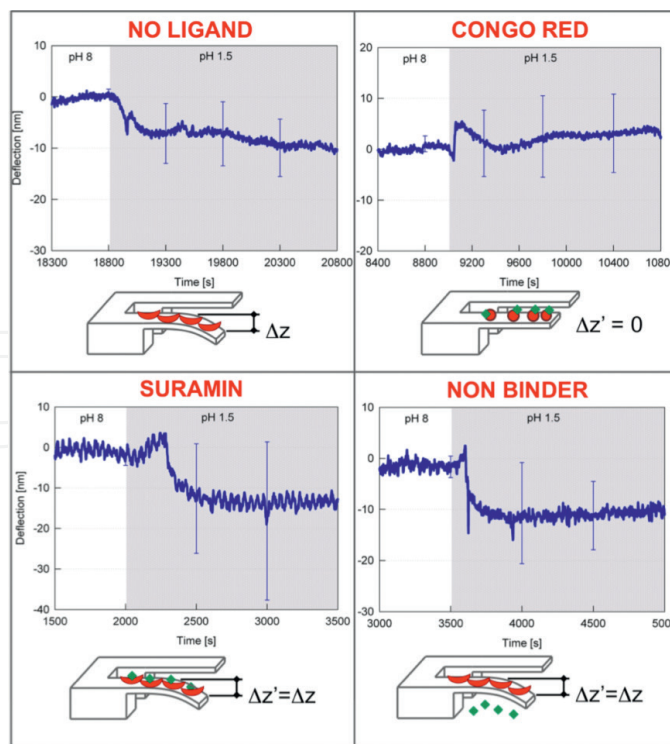


Figure 5. Experimental MC results and related binding-conformational scenarios of incubation of $\beta 2$ -m with the selected small molecule ligands. See the main text for the explanation.

activity of the selected set of small ligands, the β 2-m MCs were incubated *ex situ* in a 6 μ M solution of congo red, suramin or nonbinder (see Ref. [29] for the ligand concentration). Then, the β 2-m MCs system was exposed again to the pH switch. **Figure 5** reports the results and cartoons to explain the different binding-conformation scenarios. The β 2-m MCs incubated with congo red show no differential deflection ($\Delta z = 0$) after the pH switch. To the contrary, β 2-m MCs incubated with suramin and nonbinder drive a deflection of about -10 nm, that is compatible with the deflection of the native β 2-m MCs. MC deflection therefore indicates that only congo red is able to stabilize the β 2-m in its native conformation and prevent the conformational change upon the applied pH shift, while suramin and the nonbinder compound fail. Remarkably, it is known that suramin binds to β 2-m with the same binding affinity of congo red (in order of 10^{-5} M) [29, 30], but only congo red exerts an *in vitro* anti-amyloid activity [28], matching the nanomechanical results.

These findings demonstrate how nanomechanical sensors can be an extraordinary platform for the screening small ligands of proteins involved in pathological processes.

2.3. The nanomechanical side of ferritin iron loading

Sections 2.1 and 2.2 refer to nanomechanical biomolecular recognition driven by ligand-receptor interactions and molecular switches, where deflection is determined mostly by biomolecular conformational changes. Instead, in the following section, the study of a class of proteins with negligible conformational rearrangements is presented. In the particular case herein discussed, the surface energy change does not take origin from conformational changes, but is related to the electrostatic interaction between the inorganic new-born nanocores in ferritin cage proteins and other nonspecific short range forces, such as steric, bridging and depletion forces. These findings give the first observation on the in-plane forces arising upon ferritin iron loading confined at a solid-liquid interface [31].

Ferritin is a mineralization protein dedicated to the storage of intracellular free iron and peroxides, protecting the cell from oxidative damage [32]. Mammalian ferritin is made of 24 subunits that self-assemble in a 12 nm shell structure with an inner cavity of 8 nm in diameter able to accommodate up to about 4500 iron atoms [33]. The potential application of ferritin in the field of nanotechnology and nanomedicine [34], together with the rapid development of novel nanomaterials [35, 36], increases the need to understand and control the properties, interactions and iron loading activity of surface confined ferritin.

The rationale depicted in **Figure 6** shows a ferritin-MC assay based on recombinant human ferritin H chain (FTH) and a mutant without ferroxidase activity (Mutant). A thin film of active FTH (green circles) is deposited onto a MC, which balances by bending the variation of surface energy triggered by iron loading. A control MC is prepared by the surface functionalization with the Mutant that is not able to take up iron in the experimental conditions (light blue circles).

Figure 7a reports in dark gray line the absolute deflection of the MC modified with FTH (FTH-MC), in light gray line the absolute deflection of the reference MC modified with the

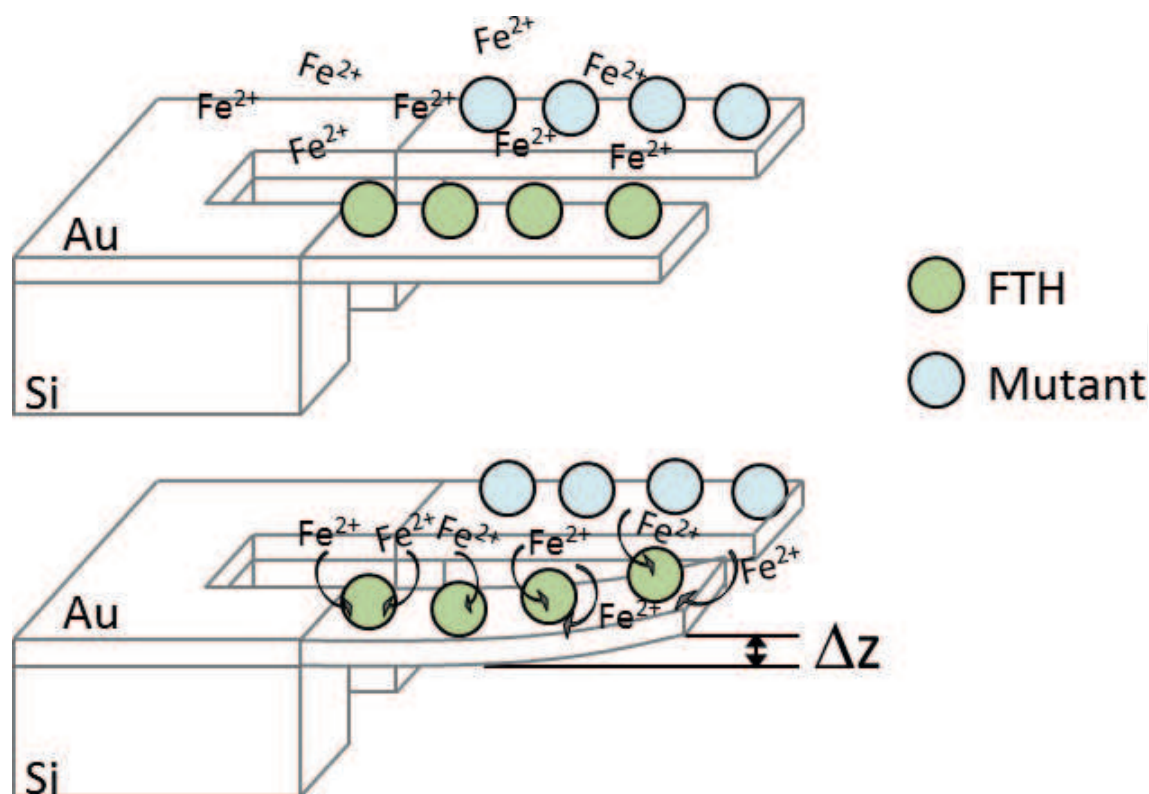


Figure 6. Cartoon depicting the ferritin-MC assay based on recombinant human ferritin H chain (FTH, green circles) and a mutant without ferroxidase activity (Mutant, light blue circles). The variation of surface energy triggered by the iron loading in FTH drives the FTH MC deflection, Δz .

Mutant (ref-MC), and in red line the differential deflection between the two signals, Δz . Vertical arrows indicate a sequential injections of Fe(II) solution necessary to reach a progressive iron loading and to limit the oxidation of nonloaded Fe(II) on the outer structure of the protein leading to Fe(III) precipitation. The presentation of Δz signal reduces any contribution to MCs deflection due to unspecific adsorption of Fe(II) and/or other components of the buffer solution. The trend depicted in **Figure 7a** is confirmed by the bar chart plot in **Figure 7b** that shows the mean equilibrium Δz over 4 replicate MC (the error bars represent the SD of the mean). The Δz value reaches a plateau value at $\Delta z = (28.1 \pm 9.6)$ nm, corresponding to a net tensile surface stress change, $\Delta\sigma = (6.0 \pm 1.5)$ mJ/m². By further calculation (see Ref. [31] for details) is possible to convert the Δz value at saturation in in-plane interferritin interactions force of about $40 k_B T$ at room temperature, coming along the formation of iron cores. This value indicates long-lived van der Waals and electrostatic interactions [37], consistent with reports on nanomechanical biomolecular recognition. Finally, by building up a purely attractive model between the iron cores, described by van der Waals (VDW) interaction potential, it comes out that the 40% of the measured energy variation of the interactions can be ascribed to VDW attractive forces between the newborn ferritin iron cores, and the remaining part ascribed to nonspecific short-range forces typical of biomolecule surface confined systems, such as hydration, steric, bridging and depletion forces [37, 38].

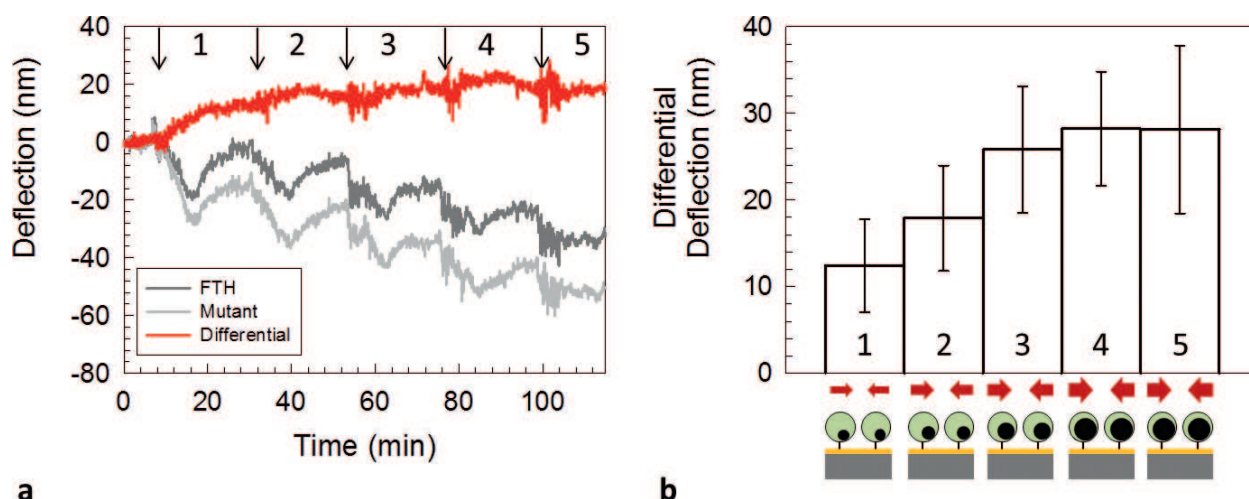


Figure 7. MC responses upon sequential injection of Fe(II). (a) Single MC deflection signals of: FTH-MC (dark gray line), ref-MC (light gray line) and differential deflection (red line). (b) Mean differential deflection, Δz , signals at equilibrium at each injection step.

3. Breaking good. Probing designer drug family with a unique supramolecular nanomechanical sensor

The systems presented in previous sections relate in general to biological systems and, in particular, to interactions of biomolecules confined at solid-solution interface, neglecting the large pool of available synthetic receptors. Nanomechanical sensors are limited, in fact, by the availability of coatings that interact selectively with the target analyte. By introducing the phosphonate cavitands as a versatile class of synthetic receptors [39] that are capable of binding inorganic and organic cations [40, 41] as well as neutral molecules [42] is possible to extend the surface nanomechanics to supramolecular systems.

Phosphonate cavitands are synthetic abiotic receptors (hosts) [39, 40, 43] with molecular recognition properties that have been exploited in gas sensing [44], supramolecular polymers [45, 46], surface self-assembly [47], and product protection [48]. They are specifically designed to target small molecules bearing amino-functionalities via a synergistic combination of weak interactions such as H-bonding, dipole-dipole, and CH- π interactions. Probing small molecules bearing amino-functionalities is a key issue from both the fundamental and the applied sides. N-Methylated moieties, in particular, are present in a broad range of biologically active compounds, from drugs [49] to cancer biomarkers [50] and neurotransmitters [51].

In the Section 3.1, we will present the preliminary study toward the viability of cavitand-MC nanomechanical sensors for probing small molecules bearing amino-functionalities. In Section 3.2, we show how we implemented these results to realize a nanomechanical device for label-free detection of amine-based illicit and designer drug in water.

3.1. Alkyl ammonium series

Figure 8 sketches a label-free selective detection of N-methyl-ammonium salts in methanol attained thanks to the use of MCs functionalized with tetraphosphonate cavitands. These molecules are LMW species of a mass equal to or lower than 150 Da, differing only by a methyl group, which is 15 Da.

The bar chart reported in **Figure 9a** shows the mean value of the deflection peaks of MCs functionalized with the cavitand. The highest interaction intensity is obtained when methylbutyl ammonium chloride is injected, $\Delta z = (-80 \pm 10)$ nm. A comparable deflection is measured with dimethylbutyl ammonium chloride and butyl ammonium chloride, with deflection values of $\Delta z = (-55 \pm 6)$ nm, and the weakest response comes from trimethyl butyl ammonium chloride, $\Delta z = (-10 \pm 2)$ nm. The trend is confirmed also by independent ITC experiments shown in **Figure 9b**. Deflection results can be read in terms of the applied surface stress driven by the host-guest complexation, determined to be $\Delta\sigma = (-17 \pm 2)$ mJ/m² for methylbutyl ammonium chloride, and $\Delta\sigma = (-12 \pm 1)$ mJ/m² for the interaction with dimethylbutyl ammonium chloride and butyl ammonium chloride. The stress was much lower for the interaction between the cavitand and the last guest, $\Delta\sigma = (-2 \pm 0.4)$ mJ/m². At the molecular level, the overall surface stress is triggered by the interplay between host-guest complexation, cavitand desolvation, and interface adsorption, as also suggested by the order of magnitude of $\Delta\sigma$, which falls in the range of intermolecular forces [52].

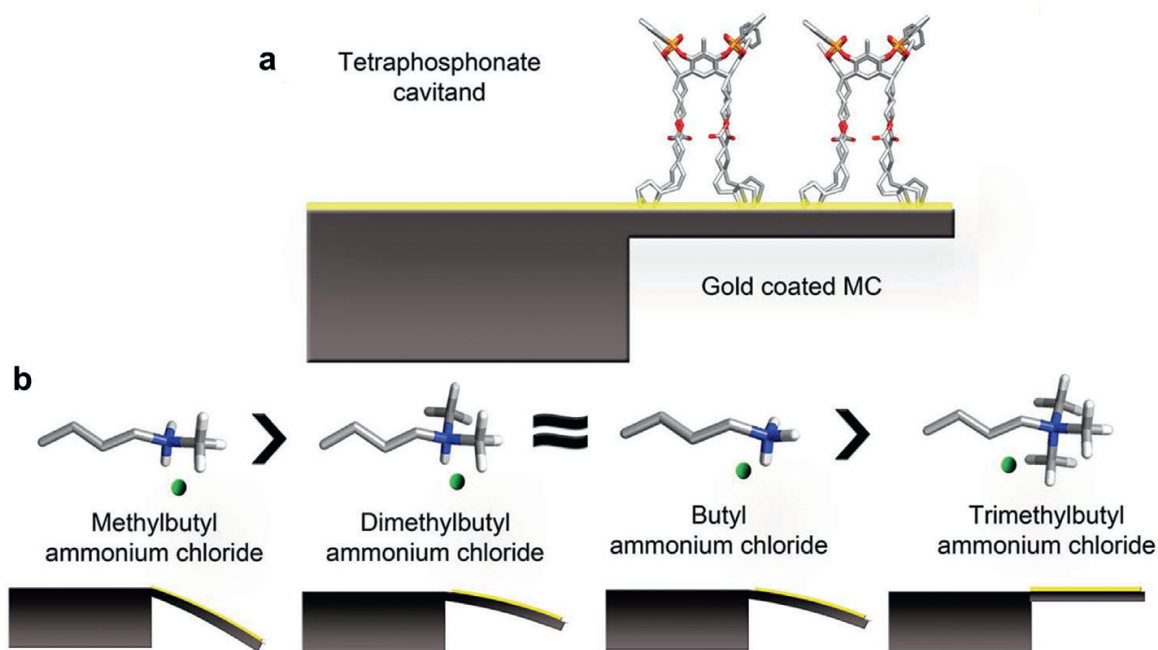


Figure 8. Scheme of the detection of N-methylammonium salts by cavitand-functionalized MCs. (a) Cavitand-MC architecture and (b) MC deflections driven by the different binding energies of N-methyl-ammonium salts and cavitands complexation.

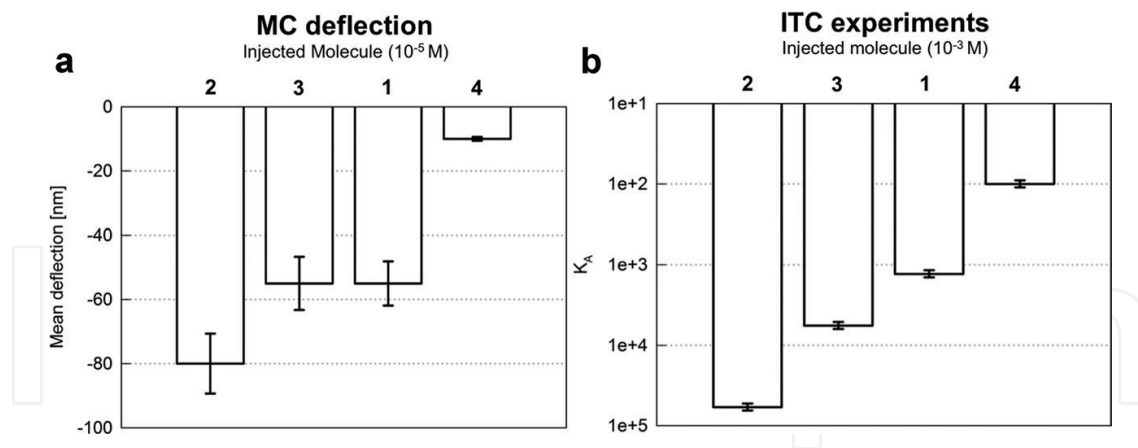


Figure 9. Bar chart of (a) the mean value of the deflection peaks of MCs functionalized with the cavitand and of (b) the mean value of K evaluated by ITC experiments.

3.2. Illicit and designer drugs

The next level application of the supramolecular nanomechanical device based on the combination of tetraphosphonate cavitands and silicon MCs depicted in previous section can be enrolled to the frontier of designer drugs identification.

Designer drugs pose serious challenges when it comes to recognizing them with the current assays, which are tailored for identification of currently illicit substances but poorly effective, or even useless, for novel designer drugs. Actually, designer variants, featuring minor modifications with respect to an existing drug, show a different chemical composition and are currently not illegal in many jurisdictions. The cavitand-MC system overcomes this shortcoming for methamphetamines, being capable to recognize the methyl-amine portion that is common to the entire drug family [53].

Data reported in **Figure 10** show the implementation of the cavitand-MC system on the detection of ecstasy (MDMA), cocaine and amphetamine in the presence of an interferent,

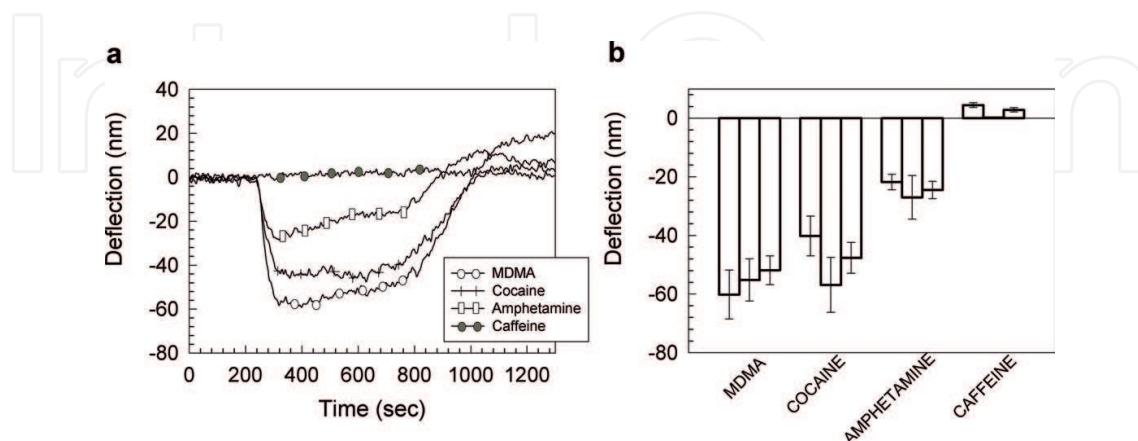


Figure 10. (a) Absolute deflection signal of cavitand-MC system upon injection of MDMA, Cocaine, Amphetamine and Caffeine and (b) mean deflection signal referring to different replicates.

such as caffeine. The different drugs drive MC responses with the same kinetics but different final equilibrium values (**Figure 10a**). Namely, the latter range from an average of 55 nm for MDMA and cocaine to 22 nm for amphetamine (with a 10% of uncertainty). The surface stress generated by the interaction gives (in modulus) $\Delta\sigma = 12 \text{ mN m}^{-1}$ for MDMA and cocaine and $\Delta\sigma = 5 \text{ mN m}^{-1}$ for amphetamine, in fully agreement with several previously reported studies, all related to biomolecules, where it is reported that recognition triggers $1 \text{ mN m}^{-1} < \Delta\sigma < 50 \text{ mN m}^{-1}$ [26, 54–56]. Other common excipients used in drug formulation, such as lactose and glucose, were investigated with the cavitand-MC system, and both MDMA and cocaine are recognized with high fidelity in the presence of the excipients [53].

Finally, the device was tested against a real “street” sample, containing 45% of 3-fluoromethamphetamine (3-FMA) and glucose as excipient. Signals reported in **Figure 11** (as absolute deflection curves in **Figure 11a** and related bar chart in **Figure 11b**) show the successful detection of the drug also directly in a real sample.

This research, that moves from advanced understanding of molecular recognition at the solid-liquid interface to complement the analytical toolbox for small molecules bearing amino functionalities, has broader horizons, including neurotransmitters and cancer biomarkers.

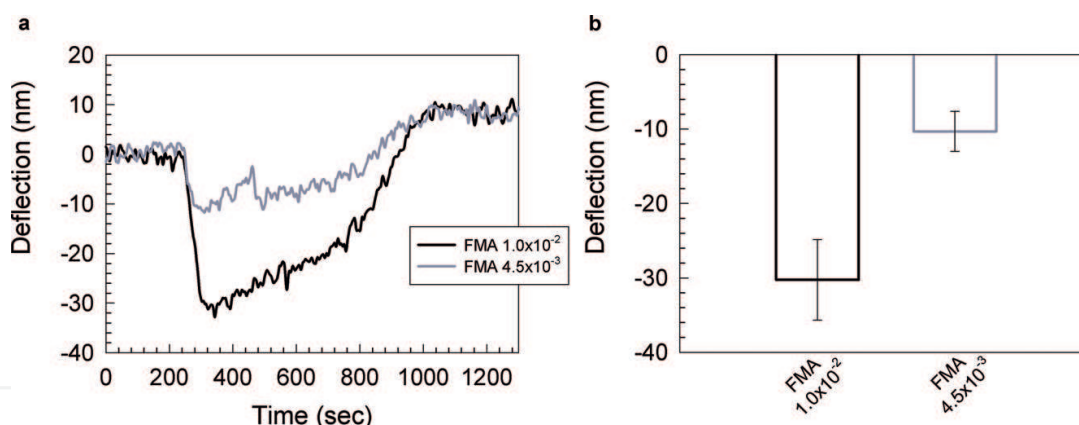


Figure 11. (a) Absolute deflection signal of cavitand-MC system upon injection of the street sample at two different concentrations and (b) mean deflection signal referring to different replicates.

Acknowledgements

The authors wish to thank all the colleagues and collaborators who participated to the presented researches; without their contribution, they would have been not just impossible, but unimaginable. Warm acknowledgments first of all to Laura E. Depero, Giulio Oliviero and Daniele Maiolo and then to Marcella Chiari, Ersilia De Lorenzi, Marco Presta, Paolo Arosio, Enrico Dalcanale Guido Condorelli and their research groups.

Author details

Paolo Bergese^{1*} and Stefania Federici²

*Address all correspondence to: paolo.bergese@unibs.it

1 Department of Molecular and Translational Medicine, INSTM, CSGI, University of Brescia, Brescia, Italy

2 Department of Mechanical and Industrial Engineering, INSTM, University of Brescia, Brescia, Italy

References

- [1] Bergese P, Oliviero G, Alessandri I, Depero LE. Thermodynamics of mechanical transduction of surface confined receptor/ligand reactions. *Journal of Colloid and Interface Science*. 2007;**316**:1017–1022. DOI: 10.1016/j.jcis.2007.08.048
- [2] Federici S, Oliviero G, Maiolo D, Depero LE, Colombo I, Bergese P. On the thermodynamics of biomolecule surface transformations. *Journal of Colloid and Interface Science*. 2012;**375**:1–11. DOI: 10.1016/j.jcis.2012.02.013
- [3] Bergese P, Colombo I. Thermodynamics of (nano) interfaces. In: Berti D, Palazzo G, editors. *Colloidal Foundations of Nanoscience*. Elsevier; 2014. pp. 1–31. ISBN: 978-0-444-59541-6
- [4] Arlett JL, Myers EB, Roukes ML. Comparative advantages of mechanical biosensors. *Nature Nanotechnology*. 2011;**6**:203-215. DOI: 10.1038/nnano.2011.44
- [5] Bergese P, Oliviero G, Colombo I, Depero LE. Molecular recognition by contact angle: Proof of concept with DNA hybridization. *Langmuir*. 2009;**25**:4271-4273. DOI: 10.1021/la900428u
- [6] Fritz J. Cantilever biosensors. *Analyst*. 2008;**133**:855–863. DOI: 10.1039/B718174D
- [7] Stoney GG. The tension of metallic films deposited by electrolysis. *Proceedings of the Royal Society A*. 1909;**83**:172–175. DOI: 10.1098/rspa.1909.0021
- [8] Carrascosa LG, Moreno M, Alvarez M, Lechuga LM. Nanomechanical biosensors: A new sensing tool. *Trends in Analytical Chemistry*. 2006;**25**:196–206. DOI: 10.1016/j.trac.2005.09.006
- [9] Álvarez M, Carrascosa LG, Moreno M, Calle A, Zaballos A, Lechuga LM, Martínez-A C, Tamayo J. Nanomechanics of the formation of DNA self-assembled monolayers and hybridization on microcantilevers. *Langmuir*. 2004;**20**:9663–9668. DOI: 10.1021/la0489559

- [10] McKendry R, Zhang J, Arntz Y, Strunz T, Hegner M, Lang HP, Bailer MK, Certa U, Meyer E, Guntherodt HJ, Gerber C. Multiple label-free biodetection and quantitative DNA-binding assays on a nanomechanical cantilever array. *Proceedings of the National Academy of Sciences USA*. 2002;**99**:9783–9788. DOI: 10.1073/pnas.152330199
- [11] Oliviero G, Federici S, Colombi P, Bergese P. On the difference of equilibrium constants of DNA hybridization in bulk solution and at the solid-solution interface. *Journal of Molecular Recognition*. 2010;**24**:182–187. DOI: 10.1002/jmr.1019
- [12] Maiolo D, Federici S, Ravelli L, Depero LE, Hamad-Schifferli K, Bergese P. Nanomechanics of surface DNA switches probed by captive contact angle. *Journal of Colloid and Interface Science*. 2013;**402**:334–339. DOI: 10.1016/j.jcis.2013.03.069
- [13] Arntz Y, Seelig JD, Lang HP, Zhang J, Hunziker P, Ramseyer JP, Meyer E, Hegner M, Gerber C. Label-free protein assay based on a nanomechanical cantilever array. *Nanotechnology*. 2003;**14**:86–90. DOI: 10.1088/0957-4484/14/1/319
- [14] Maiolo D, Mitola S, Leali D, Oliviero G, Ravelli C, Bugatti A, Depero LE, Presta M, Bergese P. Role of nanomechanics in canonical and noncanonical pro-angiogenic ligand/VEGF receptor-2 activation. *Journal of the American Chemical Society*. 2012;**134**:14573–14579. DOI: 10.1021/ja305816p
- [15] Ilic B, Yang Y, Craighead HG. Virus detection using nanoelectromechanical devices. *Applied Physics Letters*. 2004;**85**:2604–2606. DOI: 10.1063/1.1794378
- [16] Gfeller KY, Nugaeva N, Hegner M. Micromechanical oscillators as rapid biosensor for the detection of active growth of *Escherichia coli*. *Biosensors and Bioelectronics*. 2005;**21**:528–533. DOI: 10.1016/j.bios.2004.11.018
- [17] Xu A, Huang P. Receptor tyrosine kinase coactivation networks in cancer. *Cancer Research*. 2010;**15**:3857–3860. DOI: 10.1158/0008-5472
- [18] Folkman J. Angiogenesis in cancer, vascular, rheumatoid and other disease. *Nature Medicine*. 1995;**1**:27–31. DOI: 10.1038/nm0195-27
- [19] Chung AS, Lee J, Ferrara N. Targeting the tumour vasculature: Insights from physiological angiogenesis. *Nature Reviews Cancer*. 2010;**10**:505–514. DOI: 10.1038/nrc2868
- [20] Tvorogov D, et al. Effective suppression of vascular network formation by combination of antibodies blocking VEGFR ligand binding and receptor dimerization. *Cancer Cell*. 2010;**18**:630–640. DOI: 10.1016/j.ccr.2010.11.001
- [21] Ferrara N, Gerber HP, LeCouter J. The biology of VEGF and its receptors. *Nature Medicine*. 2003;**9**:669–676. DOI: 10.1038/nm0603-669
- [22] Olsson AK, Dimberg A, Kreuger J, Claesson-Welsh L. VEGF receptor signalling in control of vascular function. *Nature Reviews Molecular Cell Biology*. 2006;**7**:359–371. DOI:10.1038/nrm1911

- [23] Oliviero G, Maiolo D, Leali D, Federici S, Depero LE, Presta M, Mitola S, Bergese P. Nanoliter contact angle probes tumor angiogenic ligand–receptor protein interactions. *Biosensors and Bioelectronics*. 2010;**26**:1571–1575. DOI: 10.1016/j.bios.2010.07.115
- [24] Maiolo D, Mitola S, Leali D, Oliviero G, Ravelli C, Bugatti A, Depero LE, Presta M, Bergese P. Role of nanomechanics in canonical and noncanonical pro-angiogenic ligand/VEGF receptor-2 activation. *Journal of the American Chemical Society*. 2012;**134**:14573–14579. DOI: 10.1021/ja305816p
- [25] Rusnati M, Bugatti A, Mitola S, Leali D, Bergese P, Depero LE, Presta M. Exploiting surface plasmon resonance (SPR) technology for the identification of fibroblast growth factor-2 (FGF2) antagonists endowed with antiangiogenic activity. *Sensors*. 2009;**9**:6471–6503. DOI: 10.3390/s90806471
- [26] Federici S, Oliviero G, Hamad-Schifferli K, Bergese P. Protein thin film machines. *Nanoscale*. 2010;**2**:2570–2574. DOI: 10.1039/C0NR00616E
- [27] Merlini G, Bellotti V. Molecular mechanisms of amyloidosis. *The New England Journal of Medicine*. 2003;**349**:583–596. DOI: 10.1056/NEJMra023144
- [28] Carazzone C, Colombo R, Quaglia M, Mangione P, Raimondi S, Giorgetti S, Caccialanza G, Bellotti V, De Lorenzi E. Sulfonated molecules that bind a partially structured species of β_2 -microglobulin also influence refolding and fibrillogenesis. *Electrophoresis*. 2008;**29**:1502–1510. DOI: 10.1002/elps.200700677
- [29] Quaglia M, Carazzone C, Sabella S, Colombo R, Giorgetti S, Bellotti V, De Lorenzi E. Search of ligands for the amyloidogenic protein β_2 -microglobulin by capillary electrophoresis and other techniques. *Electrophoresis*. 2005;**26**:4055–4063. DOI: 10.1002/elps.200500313
- [30] Regazzoni L, Bertolotti L, Vistoli G, Colombo R, Aldini G, Serra M, Carini M, Caccialanza G, De Lorenzi E. A combined high-resolution mass spectrometric and insilicoapproach for the characterisation of small ligands of β_2 -microglobulin. *ChemMedChem*. 2010;**5**:1015–1025. DOI: 10.1002/cmdc.201000082
- [31] Federici S, Padovani F, Poli M, Carmona Rodriguez F, Arosio P, Depero LE, Bergese P. Energetics of surface confined ferritin during iron loading. *Colloids and Surfaces B: Biointerfaces*. 2016;**145**:520–525. DOI: 10.1016/j.colsurfb.2016.05.044
- [32] Arosio P, Levi S. Cytosolic and mitochondrial ferritins in the regulation of cellular iron homeostasis and oxidative damage. *Biochimica et Biophysica Acta*. 2010;**1800**:783–792. DOI: 10.1016/j.bbagen.2010.02.005
- [33] Chasteen ND, Harrison PM. Mineralization in ferritin: An efficient means of iron storage. *Journal of Structural Biology*. 1999;**126**:182–194. DOI: 10.1006/jsbi.1999.4118
- [34] Jutz G, van Rijn P, Santos Miranda B, Boker A. Ferritin: A versatile building block for bionanotechnology. *Chemical Reviews*. 2015;**115**:1653–1701. DOI: 10.1021/cr400011b

- [35] Knez M, Kadri A, Wege C, Gösele U, Jeske H, Nielsch K. Atomic layer deposition on biological macromolecules: Metal oxide coating of tobacco mosaic virus and ferritin. *Nano Letters*. 2006;**6**:1172–1177. DOI: 10.1021/nl060413j
- [36] Yamashita I, Iwahori K, Kumagai S. Ferritin in the field of nanodevices. *Biochimica et Biophysica Acta*. 2010;**1800**:846–857. DOI: 10.1016/j.bbagen.2010.03.005
- [37] Leckband D, Israelachvili JN. Intermolecular forces in biology. *Quarterly Reviews of Biophysics*. 2001;**34**:105–267. DOI: 10.1017/S0033583501003687
- [38] Briscoe WH. Depletion forces between particles immersed in nanofluids. *Current Opinion in Colloid & Interface Science*. 2015;**20**:46–53. DOI: 10.1016/j.cocis.2014.12.002
- [39] Pinalli R, Suman M, Dalcanale E. Cavitands at Work: From Molecular Recognition to Supramolecular Sensors. *Eur. J. Org. Chem*. 2004;2004:451–462. DOI: 10.1002/ejoc.200300430
- [40] Dutasta JP. New phosphorylated hosts for the design of new supramolecular assemblies. *Topics in Current Chemistry*. 2004;**232**:55–91. DOI: 10.1007/b13779
- [41] Vachon J, Harthong S, Jeanneau E, Aronica C, Vanthuyne N, Roussel C, Dutasta JP. Inherently chiral phosphonatecavitands as artificial chemo- and enantio-selective receptors of natural ammoniums. *Organic & Biomolecular Chemistry*. 2011;**9**:5086–5091. DOI: 10.1039/C1OB05194F
- [42] Maffei F, Betti P, Genovese D, Montalti M, Prodi L, De Zorzi R, Geremia S, Dalcanale E. Highly selective chemical vapor sensing by molecular recognition: Specific detection of C₁–C₄ alcohols with a fluorescent phosphonate cavitand. *Angewandte Chemie International Edition*. 2011;**50**:4654–4657. DOI: 10.1002/anie.201100738
- [43] Nifant'ev EE, Maslennikova VI, Merkulov RV. Design and study of phosphocavitands – A new family of cavity systems. *Accounts of Chemical Research*. 2005;**38**:108–116. DOI: 10.1021/ar0401810
- [44] Melegari M, Suman M, Pirondini L, Moiani D, Massera C, Ugozzoli F, Kalenius E, Vainiotalo P, Mulatier JC, Dutasta JP, Dalcanale E. Supramolecular sensing with phosphonate cavitands. *Chemistry – A European Journal*. 2008;**14**:5772–5779. DOI: 10.1002/chem.200800327
- [45] Yebeut'chou RM, Tancini F, Demitri N, Geremia S, Mendichi R, Dalcanale E. Host–guest driven self-assembly of linear and star supramolecular polymers. *Angewandte Chemie International Edition*. 2008;**47**:4504–4508. DOI: 10.1002/ange.200801002
- [46] Tancini F, Yebeut'chou RM, Pirondini L, De Zorzi R, Geremia S, Scherman OA, Dalcanale E. Host–guest-driven copolymerization of tetraphosphonatecavitands. *Chemistry – A European Journal*. 2010;**16**:14313–14321. DOI: 10.1002/chem.201002237
- [47] Tancini F, Genovese D, Montalti M, Cristofolini L, Nasi L, Prodi L, Dalcanale E. Hierarchical self-assembly on silicon. *Journal of the American Chemical Society*. 2010;**132**:4781–4789. DOI: 10.1021/ja9099938

- [48] Yebeutchou RM, Dalcanale E. Highly selective monomethylation of primary amines through host–guest product sequestration. *Journal of the American Chemical Society*. 2009;**131**:2452–2453. DOI: 10.1021/ja809614y
- [49] ATLAS on Substance Use (2010) – Resources for the prevention and treatment of substance use disorders; World Health Organization; 2011
- [50] Sreekumar A, et al. Metabolomic profiles delineate potential role for sarcosine in prostate cancer progression. *Nature*. 2009;**457**:910–914. DOI: 10.1038/nature07762
- [51] Von Bohlen und Halbach O, Dermietzel R. Neurotransmitters and Neuromodulators: Handbook of Receptors and Biological Effects. Weinheim: Wiley-VCH; 2006
- [52] Israelachvili JN. Intermolecular and Surface Forces, with Applications to Colloidal and Biological Systems. London: Academic Press; 1985
- [53] Biavardi E, Federici S, Tudisco C, Menozzi D, Massera C, Sottini A, Condorelli GG, Bergese P, Dalcanale E. Cavitand-grafted silicon microcantilevers as a universal probe for illicit and designer drugs in water. *Angewandte Chemie International Edition*. 2014;**53**:9183–9188. DOI: 10.1002/anie.201404774
- [54] Godin M, Tabard-Cossa C, Miyahara Y, Monga T, Williams PJ, Beaulieu LY, Lennox RB, Grutter P. Cantilever-based sensing: The origin of surface stress and optimization strategies. *Nanotechnology*. 2010;**21**:075501–075509. DOI: 10.1088/0957-4484/21/7/075501
- [55] de Puig H, Federici S, Baxamusa SH, Bergese P, Hamad-Schifferli K. Quantifying the Nanomachinery of the Nanoparticle–Biomolecule Interface. *Small*. 2011;**7**:2477–2484. DOI: 10.1002/smll.201100530
- [56] Kang K, Sachan A, Nilsen-Hamilton M, Shrotriya P. Aptamer functionalized microcantilever sensors for cocaine detection. *Langmuir*. 2011;**27**:14696–14702. DOI: 10.1021/la202067y

IntechOpen